

Non-peer-reviewed preprint

16 Recrystallization of ice enhances the creep and 17 vulnerability to fracture of ice shelves

18 Meghana Ranganathan^a, Brent Minchew^a, Colin R. Meyer^b, Matěj Peč^a

^a*Department of Earth, Atmospheric and Planetary Sciences, Massachusetts Institute of
Technology, 77 Massachusetts Ave, Cambridge, 02139, MA, USA*

^b*Thayer School of Engineering, Dartmouth College, 14 Engineering
Dr, Hanover, 03755, NH, USA*

19 **Abstract**

The initiation of fractures and fast flow in floating regions of Antarctica have the potential to destabilize large regions of the grounded ice sheet, leading to rapid sea-level rise. While observations have shown rapid, localized deformation and damage in the margins of fast-flowing glaciers, there remain gaps in our understanding of how rapid deformation affects the viscosity and toughness of ice. Here we derive a model for dynamic recrystallization of ice that includes a novel representation of migration recrystallization. This mechanism is absent from existing models and is likely dominant in warm areas undergoing rapid deformation, such as shear margins in ice sheets. While solid earth studies find fine-grained rock in shear zones, here we find elevated ice grain sizes (> 10 mm) due to warmer temperatures and high strain rates activating migration recrystallization. Large grain sizes imply that ice in shear margins deforms primarily by dislocation creep, suggesting a flow-law stress exponent of $n \approx 4$ rather than the canonical $n = 3$. Further, we find that this increase in grain size results in a decrease in tensile strength of ice by $\sim 75\%$ in the margins of glaciers. Thus, this increase in grain size

Non-peer-reviewed preprint

softens the margins of fast-flowing glaciers and makes ice shelf margins more vulnerable to fracture than previously supposed. These results also suggest the need to consider the effects of dynamic recrystallization in large-scale ice-sheet modeling.

20 *Keywords:* glaciers, fracture, recrystallization, creep

21 *PACS:* 0000, 1111

22 *2000 MSC:* 0000, 1111

23 **1. Introduction**

24 Ice shelves, the floating regions of large ice sheets, provide a significant
25 control on the evolution of ice sheets and their contributions to sea-level rise.
26 Ice shelves restrain (i.e., buttress) the upstream grounded portions of the
27 ice sheet, preventing rapid flow of grounded ice towards the ocean. Calving
28 events and dynamic thinning reduce the buttressing that ice shelves provide
29 to the grounded ice, resulting in accelerated flow and possible instability of
30 the ice sheet. Thus, a combination of ice fracture and accelerated flow may
31 play a significant role in controlling the stability of the West Antarctic Ice
32 Sheet (Thomas and Bentley, 1978; Wingham et al., 2009; Pollard et al., 2015;
33 Gudmundsson et al., 2019).

34 Fracture and flow generally occur in areas of rapid deformation, which
35 appears in the margins of fast-flowing glaciers and ice shelves (known as *shear*
36 *margins*). A significant concentration of fractures and damage on ice shelves
37 are found in the margins, which may have implications for the stability of the
38 ice shelf (Lhermitte et al., 2020). Further, the lateral shearing that occurs in
39 shear margins of grounded glaciers provides a control on flow speed and con-

Non-peer-reviewed preprint

40 tributes to the buttressing effect (MacAyeal, 1989; Ranganathan et al., 2021).
41 While this has been well-observed, there remains uncertainty in the physical
42 processes underlying fracturing and accelerated flow in shear margins.

43 Fundamentally, the creep and fracture of ice are dictated by the grain-
44 scale microstructure of the ice. It is well-known from solid earth studies that
45 the physical properties of the crystalline microstructure - including grain size
46 and grain orientation - affect the rates of creep and fracture of rocks signifi-
47 cantly (Van der Wal et al., 1993; De Bresser et al., 2001; Montési and Hirth,
48 2003) and modeling and laboratory studies have proposed similar effects in
49 ice (e.g. Currier and Schulson (1982); Cuffey et al. (2000); Goldsby and
50 Kohlstedt (2001); Hruby et al. (2020); Behn et al. (2020)). However, the
51 physics of the microstructure of ice has rarely been applied to the question
52 of how rapid deformation induces positive feedbacks on flow and how areas
53 of rapid deformation fracture. Here, we study the effect that deformation-
54 induced grain size evolution may have on flow and fracture of ice.

55 Observations show that grains are large in areas of glaciers where ice is
56 warm and being sheared. Measurements of grain size in the GRIP (Greenland
57 Ice Core Project) ice core and GISP2 (Greenland Ice Sheet Project 2) ice core
58 shows that grain sizes increase rapidly with depth near the base, where the
59 ice is frozen to the bed and thus strain rates are relatively large and the ice
60 is warm (Thorsteinsson et al., 1997; Gow et al., 1997). We would therefore
61 expect grains to be large in shear margins, where strain rates are quite high
62 (Gardner et al., 2018) and consequently the ice is warmed, sometimes to
63 the melting point, through viscous dissipation (Meyer and Minchew, 2018).
64 While there are no observations of grain size at depth in shear margins,

Non-peer-reviewed preprint

65 measurements made in shallow boreholes (Jackson and Kamb, 1997) and
66 observations of grain size in temperate glaciers (Tison and Hubbard, 2000)
67 support the suggestion that grains are likely large in shear margins.

68 Grain size influences the mechanisms of creep that allow ice to flow as
69 a viscous fluid (Goldsby and Kohlstedt, 2001). Most known creep mecha-
70 nisms, such as diffusion creep and grain-boundary sliding, have explicit and
71 well-tested grain size dependencies. On the other hand, numerous laboratory
72 experiments have shown that dislocation creep is practically independent of
73 grain size (Duval and Gac, 1980; Jacka, 1984). For grain-size-dependent
74 mechanisms, creep deformation is enhanced as grain sizes get smaller and
75 diminished as grain sizes grow. Therefore, the relative influence of disloca-
76 tion creep increases as grains grow and we may expect that areas of large
77 grain sizes will deform primarily by dislocation creep, a consideration with
78 important implications for the viscosity of ice. Ice viscosity in shear mar-
79 gins partially controls the flow speed of grounded ice and may affect the
80 buttressing of ice shelves, thus impacting ice shelf evolution.

81 Furthermore, the tendency for ice to fracture is a function of the size
82 and distribution of flaws, where stresses intensify. Larger flaw sizes tend to
83 increase the stress intensity, implying that in general, the tensile strength
84 of ice decreases as the flaw size increases. For intact or pristine ice, the
85 flaw size is set by the grain size, and therefore the tensile strength of ice
86 decreases as grain size increases, consistent with laboratory studies (Figure
87 3a) (Currier and Schulson, 1982; Nixon and Schulson, 1987, 1988). Thus, we
88 might suppose that glacier shear margins are likely to have relatively large
89 grain sizes that will decrease the tensile strength of the ice and could explain

Non-peer-reviewed preprint

90 the observations of crevassing and fracture (e.g. Lhermitte et al. (2020)).
91 Here, we derive a model for steady-state grain size in deforming glacier ice
92 to consider the effect that grain size may have on the creep and vulnerability
93 of ice to fracture in shear margins of rapidly-deforming glaciers.

94 **2. A Steady-State Grain Size Model**

95 Recrystallization processes alter the orientation and size of ice grains both
96 in the absence of and in response to deformation. While there are many
97 mechanisms of recrystallization, three main processes likely dominate the
98 evolution of grain size in ice: normal grain growth, grain-size reduction, and
99 migration recrystallization (Duval and Castelnau, 1995). Thus the net rate
100 of change in grain size can be described as the sum of the contributions from
101 all mechanisms, assuming that these mechanisms operate independently, as
102 past work has assumed (Austin and Evans, 2007):

$$\dot{d} = \dot{d}_{\text{red}} + \dot{d}_{\text{mig}} + \dot{d}_{\text{nor}} \quad (1)$$

103 where overdots represent time derivatives, \dot{d}_{nor} is the rate of change in grain
104 size due to normal grain growth, \dot{d}_{red} is the rate of change in grain size due to
105 grain-size reduction, and \dot{d}_{mig} is the rate of change in grain size due to migra-
106 tion recrystallization. We note that there are multiple proposed mechanisms
107 for grain size reduction (subgrain rotation by rotation recrystallization is well-
108 known in studies of ice (Derby and Ashby, 1987; Duval and Castelnau, 1995;
109 De La Chapelle et al., 1998; De Bresser et al., 1998; Montagnat and Duval,
110 2000), and other mechanisms include nucleation of grains by bulging) (De La

Non-peer-reviewed preprint

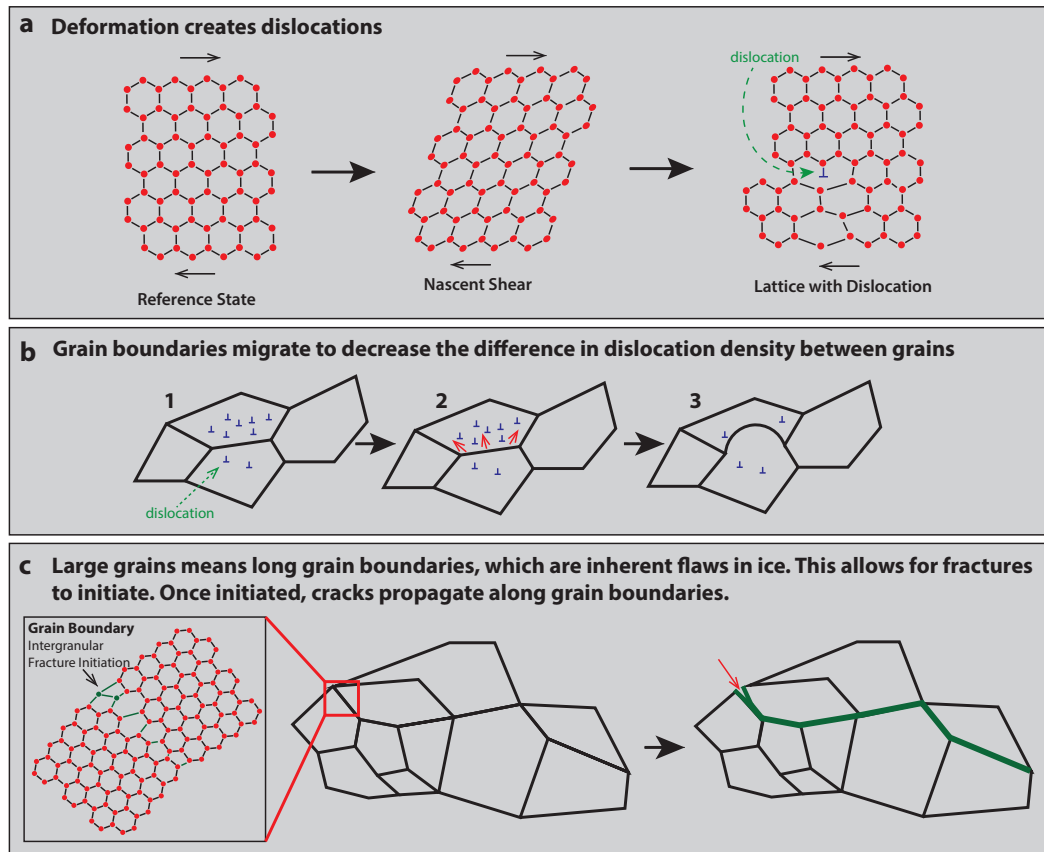


Figure 1: Schematic of migration recrystallization and its effect on ice strength. (a) In response to stress (in Antarctic glaciers, this stress arises from the ice sheet deforming under its own weight), the ice shears, creating dislocations. (b) A hypothetical polycrystalline ice of four grains. Due to local heterogeneities in stress, the density of the resulting dislocations are also heterogeneous (panel 1). To relieve stresses created by the difference in dislocation density between two grains, the grain boundary migrates towards the area of higher dislocation density (panel 2), absorbing the dislocations and leaving behind a region of zero dislocation density (panel 3). The fact that the boundary leaves behind a region of no dislocation density may create more heterogeneities in dislocation density, driving further grain boundary migration. (c) Schematic that illustrates the role grain boundaries play in fracture. This shows a theoretical polycrystalline ice of 10 grains. Grain boundaries are inherent flaws in the ice because they interrupt the ordered structure of the lattice (inset). This enables initiation of intergranular fracture in response to stresses. Once the fracture is initiated, cracks propagate along grain boundaries because they are the weakest part of the ice. Outlined in green is a potential path a fracture may take.

Non-peer-reviewed preprint

111 Chapelle et al., 1998; De Bresser et al., 2001; Rios et al., 2005; Chauve et al.,
112 2017). For many of these mechanisms, there are not explicit models or clear
113 understanding of the physical processes. In this model, we parameterize the
114 energy changes that occur during grain-size reduction and do not explicitly
115 model specific mechanisms of grain-size reduction, as previous studies have
116 done (Austin and Evans, 2007; Behn et al., 2020). Therefore, the estimates
117 presented in this study may account for multiple physical processes of grain
118 size reduction.

119 In the absence of deformation (static recrystallization), normal grain
120 growth dominates, meaning that grain boundaries migrate outwards, leading
121 to an increase in grain size (Alley, 1992). This migration is driven partially
122 by grain boundary energy γ , which represents the change in free energy
123 per change in unit area of the grain (Alley et al., 1986a,b). In contrast,
124 deformation activates the two other recrystallization mechanisms (dynamic
125 recrystallization) through the introduction of dislocations into the ice crys-
126 talline lattice. In an incompressible material such as ice, the rate of work
127 done during deformation is defined as the double inner product $\tau_{ij}\dot{\epsilon}_{ij}$ (in
128 summation notation), where τ_{ij} is the deviatoric stress tensor and $\dot{\epsilon}_{ij}$ is the
129 strain rate tensor. The work rate is a combination of the change in internal
130 energy from migration recrystallization and grain-size reduction, described
131 mathematically as

$$(1 - \Theta)\tau_{ij}\dot{\epsilon}_{ij} = \dot{E}_{\text{red}} - \dot{E}_{\text{mig}} \quad (2)$$

132 where Θ represents the fraction of the work rate that is dissipated as heat,
133 \dot{E}_{red} is the rate of change in internal energy due to grain-size reduction,

Non-peer-reviewed preprint

134 and \dot{E}_{mig} is the rate of change in internal energy due to migration recrystallization. While grain-size reduction reduces grain size, migration recrystallization grows grains: grain-scale stress gradients cause heterogeneity in dislocation density within the grain, which result in stress gradients that drive the outward migration of boundaries. This mechanism is dominant at high temperatures and high strain, where dislocation density is likely to be most heterogeneous (Duval, 1985; Alley, 1988). Since grain-size reduction and migration recrystallization have opposite effects on surface energy, the two energy rates have opposite signs (discussed more in detail in Supplement Section A).

144 Here, we build upon the steady-state grain size model from Austin and Evans (2007) by adding a parameterization for migration recrystallization, allowing us to predict grain size in shear margins. Migration recrystallization occurs when the temperature of the material approaches the melting temperature (Duval and Castelnau, 1995; Montagnat and Duval, 2000). Current steady-state grain size models, such as those derived by Derby and Ashby (1987), De Bresser et al. (1998), Hall and Parmentier (2003), and Austin and Evans (2007), were developed for solid earth studies and do not incorporate effects of migration recrystallization because rocks tend to deform at temperatures well below their melting temperatures. Ice on Earth is never more than a few tens of degrees colder than its melting temperature and thus deformation can warm ice to within a few degrees or less of its melting temperature (Meyer and Minchew, 2018), where we'd expect migration recrystallization to be most active.

Non-peer-reviewed preprint

158 *2.1. Migration Recrystallization*

159 The driving forces for migration recrystallization are the stress gradients
160 created by heterogeneities in dislocation density that drive the outward mi-
161 gration of grain boundaries (Figure 1) (Derby and Ashby, 1987). Once the
162 strain energy of grains exceeds the surface energy of the grain boundaries of
163 an individual grain, recrystallization begins in a wave from regions of high
164 strain energy and large gradients in strain energy (Duval et al., 1983; Alley,
165 1992). The grain boundaries of an individual grain migrate outwards to re-
166 duce the lattice strain energy. Recrystallization ceases when the boundary
167 energy of the grain exceeds the lattice strain energy of the grain (Duval and
168 Castelnau, 1995).

169 In this study, we derive a steady-state model and thus we consider the
170 bulk properties of a macroscopic parcel of ice, rather than any localized
171 discontinuities, when determining when migration recrystallization occurs.
172 Since strain must be accumulated to generate dislocations, previous studies
173 have assumed that this criterion is fulfilled for strains larger than 1 – 10%
174 (Duval and Castelnau, 1995). Strains of this magnitude are likely in shear
175 margins of fast-flowing glaciers and we can expect that once ice has deformed
176 sufficiently to warm the ice to -10°C , the ice has achieved strains of 1 – 10%.
177 Thus, here we let temperature be a proxy for strain and assume migration
178 recrystallization occurs for temperatures that exceed approximately -10°C ,
179 as suggested by previous works (Duval, 1981; Duval and Castelnau, 1995).

180 The temperature dependence of recrystallization kinetics are represented
181 by the activation energies. Previous studies have shown that at temperatures
182 above -10°C , the kinetics of creep and grain growth change discontinuously

Non-peer-reviewed preprint

183 due to the formation of pre-melt film and the proximity to the melting point
184 (Jacka and Li Jun, 1994; Dash et al., 2006). Here, we set the temperature
185 dependence of activation energies for creep and grain growth accordingly,
186 such that temperature plays a significant role in determining which creep
187 mechanism is dominant.

188 Ice sheet-scale shear stresses drive deformation in lateral shear margins,
189 which consequently increases the density of dislocations within grains (Figure
190 1). We can represent the driving force of migration recrystallization as the
191 difference of energy associated with a dislocation density ρ_d (defined as the
192 number of dislocations per unit surface area) between neighboring grains,
193 expressed as (Duval et al., 1983; Derby and Ashby, 1987; Derby, 1992)

$$\Delta E_{\text{dis}} = \frac{1}{2} \mu b^2 \Delta \rho_d \quad (3)$$

194 where μ is the shear modulus and b is the magnitude of the Burger's vector.
195 We express the change in dislocation density as $\Delta \rho_d \approx (\frac{D}{d})^q \rho_d$, where q is an
196 exponent to be defined, and D is the characteristic length scale over which
197 we consider the change in dislocation density. This expression is physically
198 justified by the fact that the length scale over which we consider changes
199 in dislocation density is approximately the grain size d (Duval et al., 1983;
200 Alley, 1992). The scaling of grain size by the characteristic length scale D
201 gives us a term physically comparable to strain.

202 Dislocation density has been derived by considering mechanisms that add
203 dislocations (e.g. deformation) and considering recovery mechanisms that
204 annihilate dislocations (e.g. grain-boundary movement, dislocation interac-
205 tion). Here, we consider a framework that accounts for dislocation interaction

Non-peer-reviewed preprint

206 and grain-boundary movement as recovery mechanisms and assumes that the
207 rate of dislocation addition is greater than the rate of dislocation annihila-
208 tion, which likely applies to the rapidly-deforming regions that this study
209 is considering. Assuming steady-state, dislocation density is thus found as
210 $\rho_d \approx \frac{\tau_s^2}{\mu^2 b^2}$ (Webster, 1966a,b; Duval et al., 1983; Alley, 1992; Karato, 2008).
211 Other studies have used a related framework to compute dislocation density
212 by relating the increase in dislocation density to strain-rate and comput-
213 ing the reduction in dislocation density from the area swept out by grain
214 boundaries as they migrate outwards, and these frameworks produce sim-
215 ilarly good comparisons to observations (Montagnat and Duval, 2000; Ng
216 and Jacka, 2014). While we use the former framework in thus study, as it ac-
217 counts for dislocation interactions as an annihilation mechanism, we reserve
218 for future work an in-depth exploration of these different frameworks.

219 Applying these expressions for the change in dislocation density and for
220 dislocation density to Equation 3, we can find the change in energy associated
221 with dislocation density, which is the driving force for migration recrystal-
222 lization (F_{mig}):

$$F_{mig} = \Delta E_{dis} \approx \frac{1}{2} \left(\frac{D}{d} \right)^q \frac{\tau_s^2}{\mu} \quad (4)$$

223 We can find an expression for the change of grain size by considering the
224 growth rate for grain boundary migration, which is equal to the velocity
225 of migration, $v = MF_{mig}$, where M is the mobility of the grain boundary
226 (Duval et al., 1983; Derby and Ashby, 1987; Derby, 1992). The mobility
227 of grain boundaries is expressed as $M = M_0 \exp \left[-\frac{Q_m}{RT} \right]$, where Q_m is the
228 activation energy for grain boundary mobility, R is the ideal gas constant,

Non-peer-reviewed preprint

229 T is temperature, and M_0 is the intrinsic mobility (Higashi, 1978), defined
230 here as $M_0 = 0.023 \text{ m}^4 \text{ J}^{-1} \text{ s}^{-1}$ (Llorens et al., 2017). The rate of change in
231 internal strain energy due to migration recrystallization, \dot{E}_{mig} (Equation 5),
232 is the time derivative of Equation 4, represented as

$$\dot{E}_{mig} = -\frac{1}{2} \frac{\tau_s^2}{\mu} q \frac{D^q}{d^{q+1}} \dot{d}_{mig} \quad (5)$$

$$\dot{d}_{mig} = MF_{mig} = \frac{1}{2} \frac{\tau_s^2}{\mu} \frac{D^q}{d^q} M \quad (6)$$

233 with the corresponding rate of change in grain size given by Equation 6.

234 *2.2. Normal Grain Growth*

235 The expression for the increase in grain size from normal grain growth is
236 well-established and derived from the change in surface energy that occurs
237 due to the migration of a grain boundary (Alley et al., 1986a):

$$d^p = d_0^p + kt \quad (7)$$

238 where p is the grain-growth exponent (to be constrained), d_0 is the initial
239 grain size, and k is the grain growth rate factor. The grain growth factor
240 is parameterized by $k = k_0 \exp\left[-\frac{Q_{gg}}{RT}\right]$, where k_0 is an empirical prefactor
241 and Q_{gg} is the activation energy for normal grain growth (Duval, 1985; Alley
242 et al., 1986a; Jacka and Li Jun, 1994). The rate of change in grain size due
243 to normal grain growth \dot{d}_{nor} is the time-derivative of Equation 7.

244 *2.3. Grain-size reduction*

245 Grain-size reduction increases surface energy within a volume of a polycrys-
246 talline material (Duval and Castelnau, 1995). This change in surface energy

Non-peer-reviewed preprint

247 is related to a geometric constant that represents the characteristic shape of
248 grains, grain size, and grain boundary energy γ (Alley et al., 1986a; Austin
249 and Evans, 2007). Grain boundary energy γ represents the change in free
250 energy resultant from a change in area of the grain (Derby and Ashby, 1987),
251 and laboratory experiments has found the value to be $\gamma = 0.065 \frac{\text{J}}{\text{m}^2}$ (Ketcham
252 and Hobbs, 1969). From this, the rate of change in internal energy density
253 to grain-size reduction is given as the change in surface energy, as shown in
254 Austin and Evans (2007):

$$\dot{E}_{\text{red}} = \frac{-c\gamma}{d^2} \dot{d}_{\text{red}} \quad (8)$$

255 2.4. Steady-State Grain Size

256 Grain size evolution is a function of current grain size for all three recrystallization
257 mechanisms. In the case of normal grain growth and migration
258 recrystallization, the exponents p and q respectively govern the rate of grain
259 growth. We note that both normal grain growth and migration recrystallization
260 occur by grain boundary migration. Since both recrystallization processes
261 occur by the same process, with different driving forces, the change in
262 grain size due to migration recrystallization and normal grain growth should
263 have the same grain-size dependence. To represent this condition and to
264 derive an expression for the steady-state grain size, we thus assume $q = \frac{p}{2}$.
265 We then define the expression for steady-state grain size, accounting for the
266 contribution of all mechanisms to grain size (Equation 1) and the mechanical
267 work that goes into recrystallization (Equation 2):

Non-peer-reviewed preprint

$$d_{ss} = \left[\frac{\overbrace{4kp^{-1}c\gamma\mu^2}^{\text{Normal grain growth}} + \overbrace{\tau_s^4 D^p \left(\frac{p}{2}\right) M}^{\text{Migration recrystallization}}}{\underbrace{8(1-\Theta)\tau_s\dot{\epsilon}_s\mu^2}_{\text{Grain-Size Reduction}}} \right]^{\frac{1}{1+p}} \quad (9)$$

268 where $\dot{\epsilon}_s$ is the shear strain rate. The full derivation is found in Supplement
 269 Section A. The numerator consists of both grain growth mechanisms and
 270 the denominator describes the contribution of grain reduction, similar to
 271 relations derived previously (Derby and Ashby, 1987). Without any clear
 272 estimates for Θ , we assume $\Theta \approx 1$, implying that most of the work done
 273 during deformation drives changes in thermal energy that warm the ice, a
 274 common assumption made when studying shear margins of glaciers (Jacobson
 275 and Raymond, 1998; Suckale et al., 2014; Meyer and Minchew, 2018).

276 2.5. Model Validation

277 We use GRIP ice core temperature and grain size datasets (Gundestrup
 278 et al., 1993; Thorsteinsson et al., 1997; Johnsen et al., 1997) to benchmark our
 279 model due to the availability of grain size and temperature data. In bench-
 280 marking our model against ice cores, we focus on the lower ~ 500 m of the ice
 281 column where we expect vertical shearing to be the dominant component of
 282 deformation, as these are conditions that most closely match those of shear
 283 margins and it is the region in which migration recrystallization is expected
 284 to be most active. Since the parameterizations for normal grain growth and
 285 grain-size reduction are well-established (Alley et al., 1986a,b; Austin and
 286 Evans, 2007; Behn et al., 2020), the term for migration recrystallization is
 287 the main piece of the model that requires benchmarking. Therefore, possi-

Non-peer-reviewed preprint

288 ble inconsistencies between our model setup and the conditions at shallow
289 depths (< 500 m) in GRIP do not adversely affect the comparison of our
290 model to the data.

291 The depth profile of shear strain rate and shear stress come from a nonzero
292 surface slope α , which drives ice deformation. The region of GRIP is approx-
293 imately 3 – 4 km away from an ice divide, whose position we estimated using
294 a digital elevation model (ArcticDEM; (Porter et al., 2018)) and validated
295 by previous work that used GPS data (Hvidberg et al., 1997). Close to ice
296 divides (less than an ice thickness away from the ice divide; in the case of
297 GRIP, 3 km), the strain rate is dominated by (normal) longitudinal strain,
298 whereas further away from ice divides (more than an ice thickness from the
299 divide), the strain rate becomes dominated by the vertical shear strain rate
300 due to the ice being frozen to the bed (Raymond, 1983; Gundestrup et al.,
301 1993; Hvidberg et al., 1997). Therefore, we take the vertical shear strain rate
302 to be the dominant component of the strain rate tensor in the lower portion
303 of the ice column and compute it from temperature and shear stress (Figure
304 2b). We compute vertical shear stress (taken to be equal to the gravitational
305 driving stress) for $\alpha = 0.01^\circ$ and $\alpha = 0.05^\circ$, reasonable bounds on the surface
306 slope in the region of the GRIP ice core (Helm et al., 2014). The grey shading
307 represents the depth at which the ice has not yet reached steady state (dark
308 grey for $\alpha = 0.05^\circ$, light grey for $\alpha = 0.01^\circ$), and therefore the models should
309 not predict the correct grain sizes (Figure 2c). The independence of grain
310 size model to conditions (temperature, shear strain rate, stress, grain size) at
311 all other depths (Equation 9) prevents errors at shallower depths that may
312 be attributable to unmodeled longitudinal strain rates or lack of steady state

Non-peer-reviewed preprint

313 from propagating to deeper depths, which are being used to benchmark the
314 model.

315 Our model is largely consistent with the grain size data from the GRIP ice
316 core (Figure 2c). Near the bed, migration recrystallization is the dominant
317 mechanism and thus responsible for the rapid increase in grain size. When
318 applying our model, which incorporates the contributions of migration re-
319 crystallization, we see a reasonable fit to the GRIP ice core data near the
320 bed. The depth at which grains begin to grow is largely dictated by temper-
321 ature. At temperatures of approximately -10°C , grain boundaries become
322 more mobile, enabling high-velocity grain boundary migration (Duval and
323 Castelnau, 1995; Urai et al., 1995). This critical temperature T_c at which
324 this change in activation energy occurs has been experimentally determined.
325 However, studies have shown that critical temperatures between -8°C and
326 -15°C may apply to natural conditions (Barnes et al., 1971; Goldsby and
327 Kohlstedt, 2001; Kuiper et al., 2020). We show model estimates of grain size
328 for a critical temperature of $T_c = -13^{\circ}\text{C}$ (Figure 2), to demonstrate that
329 defining a critical temperature within reasonable bounds of the canonical
330 value of -10°C produces an accurate estimate of the grain size profile. How-
331 ever, for the remainder of this study, we use the canonical value $T_c = -10^{\circ}\text{C}$
332 for consistency with much of the salient literature referenced here. We show
333 in Supplement Section B that the model provides a good fit to both GISP2
334 ice core data and WAIS Divide ice core data as well, showing that the model
335 is applicable to different ice sheets and different regions.

336 The magnitude of the change in grain size with depth is controlled primar-
337 ily by two parameters: the characteristic length-scale D and the grain growth

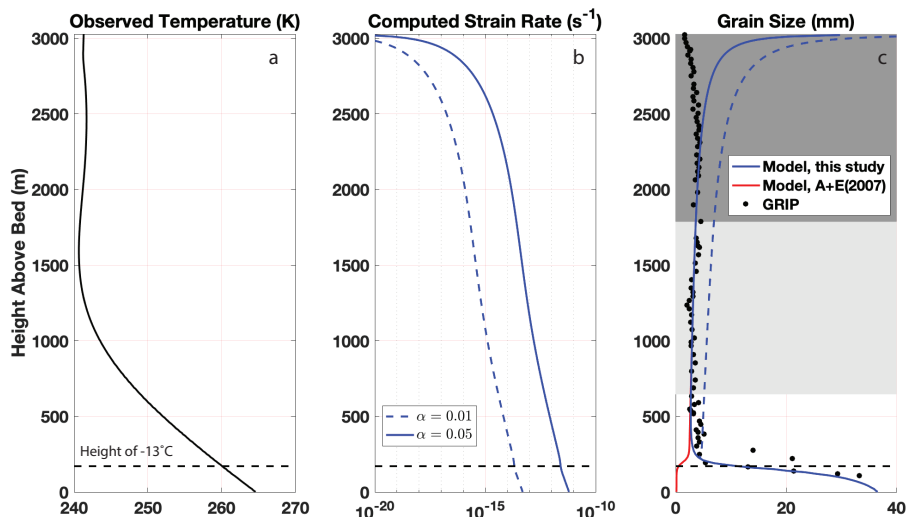


Figure 2: Results of a steady-state grain size model: (a) Temperature measured from the GRIP ice core, (b) strain rate computed from shear stress using the constitutive relation (Glen’s Flow Law) for ice (where the flow-rate parameter is found from temperature by the Arrhenius relation and the flow-law exponent is taken to be $n = 3$ (Jezek et al., 1985) for surface slopes of 0.05° (solid line) and 0.01° (dashed line), (c) grain size computed from the model presented in this study from surface slopes of 0.05° (solid blue line) and 0.01° (dashed blue line), reasonable surface slopes for this region (Helm et al., 2014), the model presented in Austin and Evans (2007) (red line), and measured from the GRIP ice core (black circles). The grey shading represents the depths at which the ice has not yet reached steady-state (dark grey for a surface slope of 0.05° and light grey for a surface slope of 0.01°) and may be contaminated by firn processes. For shear margins, the most relevant areas are those that are in steady state and thus outside the grey shaded boxes (discussed further in Supplement Section D).

Non-peer-reviewed preprint

338 exponent p (Equation 7). These two parameters are poorly constrained in
339 natural deforming glacier ice. Traditionally, the grain growth exponent is
340 taken to be $p = 2$ in glacier ice, from a fit to laboratory data and borehole
341 measurements (Duval, 1985; Alley et al., 1986a,b). Recent work has shown
342 that this value of the grain growth exponent best fits bubble-free glacier ice
343 and that bubbled ice more likely has a higher grain growth exponent (Azuma
344 et al., 2012). Since GRIP ice core is in a slowly-deforming region that is likely
345 to have a higher concentration of bubbles, we use $p = 9$ for that fit. On the
346 other hand, we are interested in rapidly-deforming regions that likely have
347 a low concentration of bubbles, so we use $p = 2$ for the remainder of this
348 study. We reserve for future work a complete exploration of the effect of
349 varying grain growth exponents. The characteristic grain size D is uncertain
350 as well, given that this is a scaling factor and the average grain size can vary
351 widely in different parts of Antarctica. In the Supplement Section C, we
352 show that values of D between 50 mm and 100 mm best represent the ice
353 core data we use here, and we take $D = 50$ mm to approximate the best fit.

354 **3. Model Results in Shear Margins**

355 We first apply this model to a single column of an idealized shear margin
356 in which the strain rate is constant with depth. We compute grain size
357 from three different strain rates, representing a reasonable range of strain
358 rates seen in shear margins of Antarctic ice streams (Alley et al., 2018).
359 We compute ice temperature from strain rate using the thermomechanical
360 model developed by Meyer and Minchew (2018) (Figure 3b) (with vertical
361 accumulation accounted for in the Peclet number, where $Pe = 2$).

Non-peer-reviewed preprint

362 For a low strain rate ($\dot{\epsilon} = 6 \times 10^{-10} \text{ s}^{-1}$), temperature increases only
363 slightly with depth and thus grain size remains relatively constant with depth.
364 For an intermediate strain rate ($\dot{\epsilon} = 1.3 \times 10^{-9} \text{ s}^{-1}$), comparable to that found
365 in shear margins of most ice streams in Antarctica, temperature increases
366 significantly with depth, reaching the melting temperature approximately
367 100 m from the bed. Grains grow with depth until the critical temperature
368 of -10°C , where there is a decrease in grain sizes due to an increase in the
369 prevalence of grain-size reduction. There is then a rapid growth of grains
370 due to temperatures approaching -10°C , when enough strain energy has
371 built for grain boundaries to migrate through migration recrystallization.
372 Below approximately 500 meters above the bed, grain sizes become roughly
373 constant with depth due to strain rate and temperature increasing enough
374 such that creep and subsequent grain reduction becomes more active and
375 balances the contribution of migration recrystallization. For a high strain rate
376 ($\dot{\epsilon} = 6 \times 10^{-8} \text{ s}^{-1}$), temperatures increase dramatically, reaching the melting
377 point approximately 700 m above the bed. The ice remains temperate for the
378 remainder of the ice column. Due to the dramatic increase in temperature
379 in the first few hundred meters, grain size increases from $\sim 2 \text{ mm}$ at the
380 surface to $\sim 13 \text{ mm}$ approximately 200 m from the surface. Grain sizes then
381 remain roughly constant with depth for the remainder of the ice column. The
382 estimate that grains are large in shear margins and regions where the ice is
383 warm is supported by observations from Antarctic ice streams (Jackson and
384 Kamb, 1997) and from temperate glaciers (Tison and Hubbard, 2000).

385 In contrast to our results, studies in the solid earth community have con-
386 sidered the effect of recrystallization on grain sizes in shear zones and found

Non-peer-reviewed preprint

387 that grain size reduces in shear zones due to the dominance of grain-size
388 reduction in regions with high strain rate (e.g. De Bresser et al. (2001);
389 Montési and Hirth (2003)). Rocks in deformational zones are often far be-
390 low their melting temperature, so a temperature increase by shear heating
391 would have to be much larger than that for ice, which is everywhere close
392 to its melting temperature. Ice temperatures near the melting point drive
393 migration recrystallization on Earth, which results in a growth in grains in
394 shear margins rather than a reduction in grain size.

395 *3.1. Effect of Grain Size on Ice Rheology*

396 Grain size affects the rheology of ice. Typically, ice rheology is described
397 through a power-law relationship (Glen’s flow law), which relates strain rate
398 to stress raised to a power n , $\dot{\epsilon} = A\tau^n$. The value of n reflects the creep
399 mechanism that ice deforms by and thus the choice of n in ice-flow model-
400 ing significantly affects the behavior of deforming ice. Uncertainties in the
401 parameters of this flow law contribute significantly to uncertainties in large-
402 scale ice-flow modeling, and constraining values of n is critical to making
403 projections of ice sheet behavior.

404 Values of $n = 3$ are commonly used because this value fits laboratory
405 data for the creep of ice (Jezek et al., 1985). However, a value of $n = 3$ does
406 not clearly match with one creep mechanism. Instead, a flow law exponent
407 of $n \approx 3$ may describe creep by a combination of dislocation creep ($n \approx 4$),
408 which is grain-size-independent, and grain-boundary sliding ($n \approx 2$), which is
409 grain-size-dependent (Montagnat and Duval, 2000; Goldsby and Kohlstedt,
410 2001; Behn et al., 2020). Deformation of ice with large grain sizes generally
411 favors dislocation creep as the dominant deformation mechanism.

Non-peer-reviewed preprint

412 Dislocation creep occurs through dislocations, line defects in the ice,
413 which enable planes of the ice crystalline lattice to move past each other.
414 Migration recrystallization annihilates dislocations through the migration of
415 grain boundaries, further increasing grain size and producing space for new
416 dislocations to move through, which allows for continued dislocation creep.
417 The rate of creep for grain-size-dependent deformation mechanisms (all ex-
418 cept dislocation creep) is inversely related to grain size, so in ice with large
419 grains, the rate of grain-size-dependent creep is likely to be low. Thus, as
420 grains grow, the flow law tends to a power-law relationship with $n = 4$,
421 describing dislocation creep as the sole creep mechanism.

422 This suggests that in areas of rapid deformation, such as the margins of
423 ice streams, modeling ice flow with a flow-law exponent of $n \approx 4$ (dislocation-
424 creep-dominant flow) may more accurately capture the dynamics occurring
425 as the ice deforms, a result also estimated using satellite observations of ice
426 shelves (Millstein and Minchew, 2020). In Supplement Section C, we show
427 these results from our model for varying values of n . The value of n directly
428 affects the rate of flow of ice, as viscosity scales with strain rate to the power
429 of $\frac{1-n}{n}$. Thus, a value of $n = 4$ implies a lower viscosity for a given strain
430 rate, suggesting that models may be overestimating the viscosity of ice in
431 areas of rapid deformation.

432 *3.2. Effect of grain size on fracture vulnerability*

433 In the absence of pre-existing macro-scale fractures, the size of grains
434 has a significant effect upon the strength of ice because grain boundaries are
435 themselves flaws in the ice along which cracks can propagate (Schulson and
436 Hibler, 1991). Intuitively, an increase in grain size translates to an increase

Non-peer-reviewed preprint

437 in the length of grain boundaries, resulting in an increase in vulnerability
438 to fracture (Figure 3a). Laboratory studies have similarly found that the
439 tensile strength of ice σ_t , defined as the total stress required to fracture ice
440 in tension, decreases with increasing grain size according to the following
441 relationship: (Currier and Schulson, 1982; Schulson et al., 1984; Nixon and
442 Schulson, 1988)

$$\sigma_t = Kd^{-\frac{1}{2}} \quad (10)$$

443 where K is a constant. While this is an empirical relationship, studies have
444 developed theoretical bases for this relationship. The most prevalent ex-
445 planation is the dislocation pileup mechanism, which explains deformation
446 through the pileup of dislocations at the edge of a grain that then induces
447 deformation in a neighboring grain (Li and Chou, 1970). Fractures initiate
448 to reduce the stress that forms due to this dislocation pileup. The stress
449 required for this to occur has the same grain size dependence as that in
450 Equation 10 (Li and Chou, 1970; Schulson et al., 1984).

451 We apply Equation 10 to compute the tensile strength of ice as a function
452 of grain size (setting $K = 52 \text{ kPa m}^{\frac{1}{2}}$ (Lee and Schulson, 1988)) for the
453 case of the idealized shear margin (Figure 3b). For a low strain rate, since
454 grain sizes remain approximately constant with depth, tensile strength also
455 remains roughly constant with depth and $\sigma_t \approx 1.2 \text{ MPa}$. For an intermediate
456 strain rate, grain sizes grow between approximately 400 and 600 m above
457 the bed before reaching a steady-state grain size of approximately 15 mm
458 and then remaining constant with depth for the remainder of the ice column.
459 Similarly, tensile strength remains constant until approximately 600 m above

Non-peer-reviewed preprint

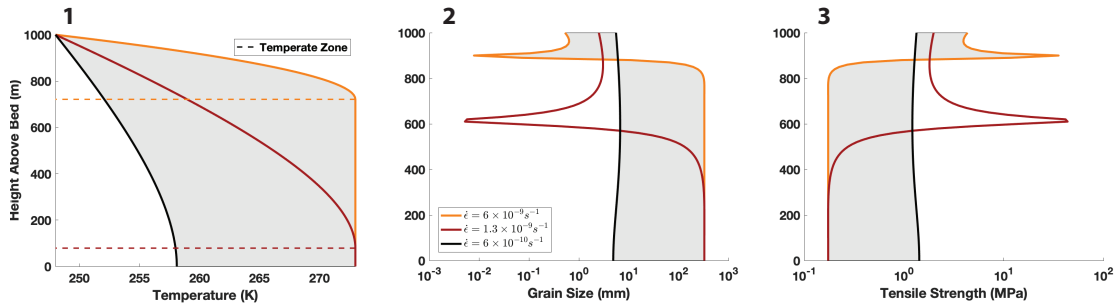


Figure 3: Results from an idealized model showing the relationship between ice temperature, grain size, and tensile strength. (1) Ice temperature computed from the thermomechanical model presented in Meyer and Minchew (2018), (2) Grain size computed from the steady-state grain size model developed here (Equation 9), (3) Tensile strength computed from Equation 10, for 3 strain rates.

460 the bed. At this depth, tensile strength increases sharply due to a decrease
 461 in grain size, and then tensile strength decreases to approximately 0.4 MPa
 462 and remains constant with depth to the bed. At a high strain rate, tensile
 463 strength follows a similar pattern as that for intermediate strain rates, though
 464 the decrease in tensile strength occurs closer to the surface (~ 900 m height).

465 In locations of ice sheets in which the ice is frozen to the bed, a similar
 466 decrease in tensile strength will be likely near the bed due to an increase
 467 in grain size caused by migration recrystallization, as seen in the GRIP ice
 468 core (Figure 2). However, that decrease in tensile strength would be coupled
 469 with an increase in the overburden pressure, preventing tensile fractures from
 470 forming. In the case of shear margins, however, we observe a decrease in
 471 tensile strength to approximately 25% of the tensile strength a few hundreds
 472 of meters below the surface. With relatively low overburden pressure at these
 473 depths, this leaves a significant depth of the shear margin vulnerable to the

Non-peer-reviewed preprint

474 propagation of microcracks along grain boundaries and thus the nucleation
475 of large-scale fractures. Though not explicitly represented in these models,
476 we would expect the water pressure at the base of ice shelves to facilitate the
477 opening of tensile fractures, which renders the deeper portions of the shear
478 margins on ice shelves, where tensile strength is lowest, quite vulnerable to
479 fracture.

480 **4. Application to Pine Island Glacier, West Antarctica**

481 We apply our model to Pine Island Glacier in West Antarctica because
482 of its rapid deformation and potential for large-scale implications for the
483 Antarctic Ice Sheet (Wingham et al., 2009). The yearly velocity of Pine Is-
484 land Glacier is found from LANDSAT 8 satellite imagery (Figure 4b) (Gard-
485 ner et al., 2018), ice thickness is calculated from basal topography from
486 BedMachine (Morlighem et al., 2020), and surface elevation from the Ref-
487 erence Elevation Model of Antarctica (Howat et al., 2019). We use surface
488 mass balance, averaged over the years 1979-2019, from the RACMO model
489 of Antarctica to set the rate of vertical advection in the thermomechanical
490 model (Van Wessem et al., 2014). Results for other outlet glaciers in
491 Antarctica are shown in Supplement Section F.

492 We compute grain size from surface strain rates (calculated from surface
493 velocity; Figure 4b), ice temperature (calculated from surface strain rates),
494 and ice thickness. Grain size is also dependent upon Θ , the fraction of work
495 dissipated as heat. Commonly, it is assumed that all the work done during
496 deformation is dissipated as heat, $\Theta \approx 1$ (Jacobson and Raymond, 1998;
497 Suckale et al., 2014; Meyer and Minchew, 2018). However, the value has not

Non-peer-reviewed preprint

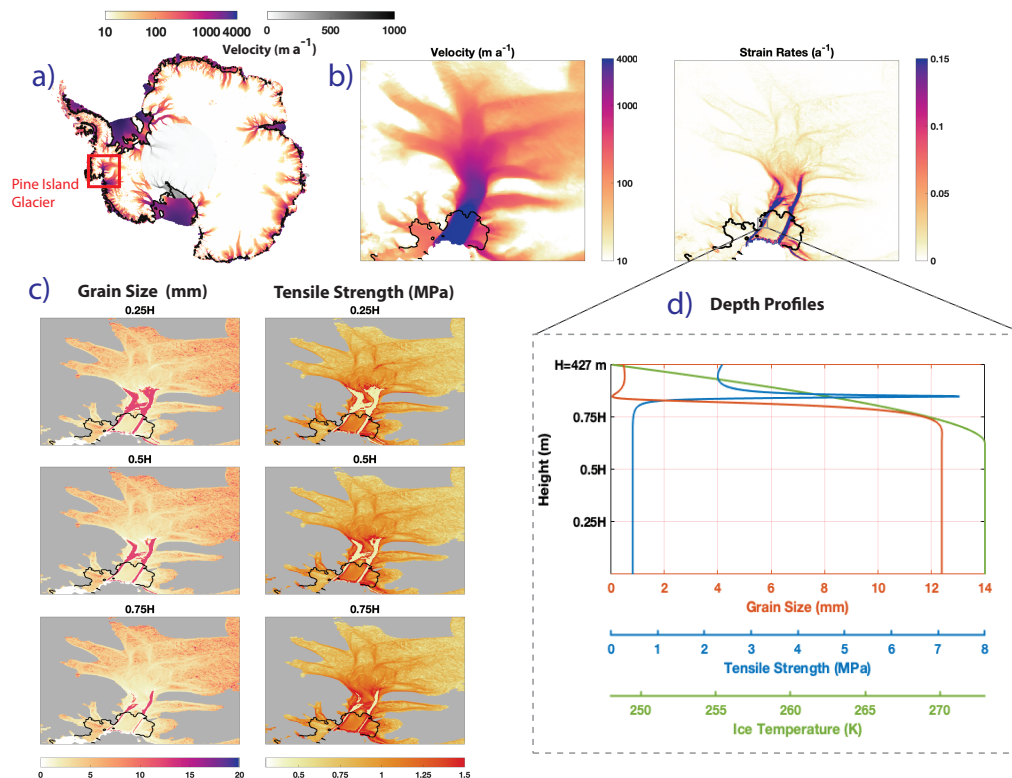


Figure 4: (a) Surface velocity of Antarctica from Landsat 7 and 8 (yellow to purple scale bar) (Gardner et al., 2018), with the pole hole filled in from NASA MEaSUREs (grey scale bar) (Mouginot et al., 2012; Rignot et al., 2017), with the region of Pine Island Glacier outlined in red. (b) Surface velocity and surface strain-rates of Pine Island Glacier. (c) Estimated grain sizes and tensile strength at varying depths: 25% of ice thickness (H) from the bed, 50% of ice thickness from the bed, and 75% of ice thickness from the bed. Areas where the model is not valid (flow speed $< 30 \text{ m a}^{-1}$) are shown in grey. Here we show results for $\Theta \approx 1$, the assumption used in thermomechanical models of ice (Jacobson and Raymond, 1998; Suckale et al., 2014; Meyer and Minchew, 2018). Results using other values of Θ are shown in Supplement Section F. (d) Depth profiles of grain size, tensile strength, and ice temperature for a single point of the shear margin of the Pine Island Glacier ice shelf.

Non-peer-reviewed preprint

498 been experimentally or theoretically constrained. Here, we present results
499 for $\Theta \approx 1$ and in the Supplement Section F we present results with $\Theta = 0.5$
500 and $\Theta = 0.25$. The tensile strength of ice is then computed from grain size.
501 We show three slices of the ice column: the grain size and tensile strength
502 at 25% of the ice thickness, at 50% of the ice thickness, and 75% of the ice
503 thickness (Figure 4c).

504 Grains are large in the shear margins of Pine Island Glacier (~ 12 mm)
505 relative to the rest of the glacier and ice core data. This is likely due to high
506 strain rates resulting in elevated ice temperatures (at or near the melting
507 point). Previous studies show extensive zones of temperate ice in the shear
508 margins of Pine Island Glacier (Meyer and Minchew, 2018), and this drives
509 migration recrystallization and increases the size of grains. The depth profile
510 largely mirrors that seen in the idealized case (Figure 3b): at the bed, most
511 of the margin contains coarse-grained ice. A similar area of coarse-grained
512 ice exists at 25% of the ice thickness. In the middle of the ice column (50%),
513 the area of coarse-grained ice thins but still spans a significant portion of the
514 margin, especially upstream. Finally, near the surface (75% of ice thickness),
515 the area of large grains thins even more but still dominates the shear margin
516 (Figure 4c,d). In general, as seen in Figure 4d, grain sizes remain constant
517 with depth beyond the region near the surface and therefore the profiles in
518 Figure 4c show the region of grain growth expanding as temperatures increase
519 with depth. The difference between grain size in the margins and grain size in
520 the trunk of the ice stream decreases as Θ decreases (as less work is dissipated
521 as heat). Even at low Θ , grains are still larger in the margins (Supplement
522 Section F). This may imply that, in the margins, dislocation creep is the

Non-peer-reviewed preprint

523 dominant deformation mechanism and thus modeling the evolution of Pine
524 Island Glacier using $n = 4$ in the margins is most accurate.

525 Large grain sizes in the margins translate to relatively low values of tensile
526 strength. Tensile strength drops from ~ 1.5 MPa in the fine-grained regions
527 to ~ 0.2 MPa in the coarse-grained regions. These values are significantly
528 lower than some estimated tensile strength values for relatively pristine and
529 undeformed ice (Ultee et al., 2020) and within the range of reasonable values
530 found by other studies (Vaughan, 1993). Furthermore, there is a significant
531 portion of the shear margin that has very low tensile strength near the surface
532 (75% of ice thickness). A reduction in tensile strength occurs for low values
533 of Θ as well, though the reduction is not as significant and does not extend as
534 far up the ice column (Supplement Section F). This dramatic drop in tensile
535 strength, particularly near the surface, may increase the vulnerability of the
536 shear margin to fracture and is positioned approximately where significant
537 damage and fracturing in Pine Island Glacier have been observed (Lhermitte
538 et al., 2020). Ice shelves are particularly vulnerable to changes in tensile
539 strength because basal crevasses are more easily formed than in grounded ice
540 due to the fact that the cracks are water-filled. A reduction in the strength of
541 ice at the base of the ice column may increase the vulnerability of ice shelves
542 significantly relative to grounded ice since it allows for cracks to propagate
543 from the base of the ice shelf and may allow for full-thickness fractures to
544 develop. This drop in tensile strength is due to the rate of deformation
545 in shear margins, and so as Pine Island Glacier accelerates in a changing
546 climate, the ice shelf of Pine Island Glacier may become more vulnerable to
547 fracture and calving events (Wingham et al., 2009).

548 5. Conclusions

549 In this study, we show that grain sizes in shear margins are large relative
550 to slower deforming regions, which influences the rate of creep and vulner-
551 ability to fracture of the ice and may contribute to accelerated flow and
552 instability of ice shelves. To show this, we derive a new model for steady-
553 state grain size that accounts for migration recrystallization, a mechanism
554 for recrystallization that is dominant at high strain rate and high tempera-
555 ture and results in an increase in grain size. Our model demonstrates that
556 migration recrystallization is dominant in shear margins and thus ice grains
557 in shear margins are large (~ 12 mm), compared to grain sizes of $\sim 2 - 7$ mm
558 in surrounding regions. This is a significant deviation from previous work in
559 solid earth recrystallization studies that have shown shear zones of rock to
560 be fine-grained. This distinction arises because ice in terrestrial glaciers and
561 ice sheets is close to its melting temperature and thus there is enough heat
562 to allow migration recrystallization to outpace grain-size reduction, resulting
563 in coarse grains in shear zones. Further, this model produces predictions of
564 grain size that can be tested by observations of grain size in shear margins.
565 We show here that this result has implications for the vulnerability of shear
566 margins to fracture and the rheology of ice in shear margins.

567 The flow of ice is described by a constitutive relation that relates strain
568 rate and stress through a power law, with a stress exponent n . The value
569 of $n = 3$ has been found to match laboratory data and is commonly used
570 in ice sheet and ice flow models. However, we suggest here that in shear
571 margins where grain sizes are large, dislocation creep ($n = 4$) is likely to be
572 the dominant deformation mechanism, since large grain sizes give more area

Non-peer-reviewed preprint

573 for slip to occur through dislocations and large grain sizes also reduce the
574 rates of creep by mechanisms such as grain-boundary sliding and diffusion
575 creep. This may imply that, by using the traditional Glen’s flow law with
576 $n = 3$ in large-scale ice flow models, we are underestimating the rate of
577 creep, and consequently the acceleration of flow, in key regions of Antarctica.
578 Further, it is well known that an increase in grain size reduces the strength
579 of polycrystalline materials. Here, we show that the tensile strength of ice in
580 shear margins of Pine Island Glacier, West Antarctica are approximately 25%
581 of the tensile strength of ice in the centerline of the glacier. This decrease in
582 tensile strength may give rise to damage and fracture that previous studies
583 have identified in Pine Island Glacier (Lhermitte et al., 2020).

584 This new understanding of recrystallization in shear zones may provide
585 a way to estimate more accurately the vulnerability of rapidly deforming
586 glaciers to instability by parameterizing the effect of dynamic recrystalliza-
587 tion processes in large-scale ice flow models. This work provides inroads into
588 thinking about how to represent different types of flow in large-scale ice flow
589 models with a spatially varying stress exponent n . Finally, this work sug-
590 gests that dynamic recrystallization processes significantly affect the physical
591 properties and dynamics of rapidly-deforming glaciers, and further work will
592 consider the role that dynamic recrystallization and grain-scale processes play
593 in the large-scale dynamics and energetics of shear margins.

594 **Acknowledgements**

595 We acknowledge enlightening conversations and feedback from Maurine
596 Montagnat, Brian Evans, and Mark Behn, along with feedback from the MIT

Non-peer-reviewed preprint

597 Glaciers Group. M.I.R. gratefully acknowledges funding from the Martin Fel-
598 lowship and the Sven Treitel Fellowship. B.M. acknowledges funding from
599 two NSF-NERC grants, award numbers 1739031 and 1853918, and a grant
600 from the NEC Corporation Fund for Research in Computers and Computa-
601 tion. No new data were produced for this study, and data used in this study
602 are publicly available through their respective publications, cited here. The
603 code for the model and that generates the figures in this paper can be found
604 at: <https://github.com/megr090/grain-size-tensile-strength-model>.

605 **References**

606 Alley, K.E., Scambos, T.A., Anderson, R.S., Rajaram, H., Pope, A., Ha-
607 ran, T.M., 2018. Continent-wide estimates of Antarctic strain rates from
608 Landsat 8-derived velocity grids. *Journal of Glaciology* 64, 321–332.
609 doi:10.1017/jog.2018.23.

610 Alley, R., 1988. Fabrics in Polar Ice Sheets: Development and Prediction.
611 *Science* 240, 493–495. URL: [https://www.sciencemag.org/lookup/doi/](https://www.sciencemag.org/lookup/doi/10.1126/science.240.4851.493)
612 [10.1126/science.240.4851.493](https://www.sciencemag.org/lookup/doi/10.1126/science.240.4851.493), doi:10.1126/science.240.4851.493.

613 Alley, R., 1992. Flow-law hypotheses for ice-sheet modeling. *Journal of*
614 *Glaciology* 38, 245–256. URL: [https://www.cambridge.org/core/](https://www.cambridge.org/core/product/identifier/S0022143000003658/type/journal%7B%7Darticle)
615 [product/identifier/S0022143000003658/type/journal{_}article](https://www.cambridge.org/core/product/identifier/S0022143000003658/type/journal%7B%7Darticle),
616 doi:10.3189/S0022143000003658.

617 Alley, R., Perepezko, J., Bentley, C., 1986a. Grain Growth in Polar
618 Ice: I. Theory. *Journal of Glaciology* 32, 425–433. doi:10.3189/
619 s0022143000012132.

Non-peer-reviewed preprint

- 620 Alley, R., Perepezko, J., Bentley, C., 1986b. Grain Growth in Polar Ice:
621 II. Application. *Journal of Glaciology* 32, 425–433. URL: [https://www.
622 cambridge.org/core/product/identifier/S0022143000012132/type/
623 journal_article](https://www.cambridge.org/core/product/identifier/S0022143000012132/type/journal_article), doi:10.3189/S0022143000012132.
- 624 Austin, N.J., Evans, B., 2007. Paleowattmeters: A scaling re-
625 lation for dynamically recrystallized grain size. *Geology* 35,
626 343. URL: [https://pubs.geoscienceworld.org/geology/article/35/
627 4/343-346/129818](https://pubs.geoscienceworld.org/geology/article/35/4/343-346/129818), doi:10.1130/G23244A.1.
- 628 Azuma, N., Miyakoshi, T., Yokoyama, S., Takata, M., 2012. Impeding
629 effect of air bubbles on normal grain growth of ice. *Journal of Struc-
630 tural Geology* 42, 184–193. URL: [http://dx.doi.org/10.1016/j.
631 jsg.2012.05.005](http://dx.doi.org/10.1016/j.jsg.2012.05.005)[https://linkinghub.elsevier.com/retrieve/pii/
632 S019181411200123X](https://linkinghub.elsevier.com/retrieve/pii/S019181411200123X), doi:10.1016/j.jsg.2012.05.005.
- 633 Barnes, P., Tabor, D., Walker, J.C.F., 1971. The friction and creep
634 of polycrystalline ice. *Proceedings of the Royal Society of London.
635 A. Mathematical and Physical Sciences* 324, 127–155. URL: [https://
636 royalsocietypublishing.org/doi/10.1098/rspa.1971.0132](https://royalsocietypublishing.org/doi/10.1098/rspa.1971.0132), doi:10.
637 1098/rspa.1971.0132.
- 638 Behn, M.D., Goldsby, D.L., Hirth, G., 2020. The role of grain-size evolu-
639 tion on the rheology of ice: Implications for reconciling laboratory creep
640 data and the Glen flow law. *The Cryosphere Discussions* , 1–31 URL:
641 <https://tc.copernicus.org/preprints/tc-2020-295/>, doi:10.5194/
642 tc-2020-295.

Non-peer-reviewed preprint

- 643 Chauve, T., Montagnat, M., Barou, F., Hidas, K., Tommasi, A., Main-
644 price, D., 2017. Investigation of nucleation processes during dynamic re-
645 crystallization of ice using cryo-EBSD. *Philosophical Transactions of the*
646 *Royal Society A: Mathematical, Physical and Engineering Sciences* 375.
647 doi:10.1098/rsta.2015.0345.
- 648 Cuffey, K.M., Thorsteinsson, T., Waddington, E.D., 2000. A renewed argu-
649 ment for crystal size control of ice sheet strain rates. *Journal of Geophysical*
650 *Research: Solid Earth* 105, 27889–27894. URL: [http://doi.wiley.com/](http://doi.wiley.com/10.1029/2000JB900270)
651 [10.1029/2000JB900270](http://doi.wiley.com/10.1029/2000JB900270), doi:10.1029/2000JB900270.
- 652 Currier, J., Schulson, E., 1982. The tensile strength of ice as a func-
653 tion of grain size. *Acta Metallurgica* 30, 1511–1514. URL: [https://](https://linkinghub.elsevier.com/retrieve/pii/0001616082901717)
654 linkinghub.elsevier.com/retrieve/pii/0001616082901717, doi:10.
655 [1016/0001-6160\(82\)90171-7](https://doi.org/10.1016/0001-6160(82)90171-7).
- 656 Dash, J.G., Rempel, A.W., Wettlaufer, J.S., 2006. The physics of premelted
657 ice and its geophysical consequences. *Reviews of Modern Physics* 78, 695–
658 741. doi:10.1103/RevModPhys.78.695.
- 659 De Bresser, J., Ter Heege, J., Spiers, C., 2001. Grain size reduction by
660 dynamic recrystallization: can it result in major rheological weakening?
661 *International Journal of Earth Sciences* 90, 28–45. URL: [http://link.](http://link.springer.com/10.1007/s005310000149)
662 [springer.com/10.1007/s005310000149](http://link.springer.com/10.1007/s005310000149), doi:10.1007/s005310000149.
- 663 De Bresser, J.H.P., Peach, C.J., Reijs, J.P.J., Spiers, C.J., 1998. On dynamic
664 recrystallization during solid state flow: Effects of stress and temperature.

Non-peer-reviewed preprint

665 Geophysical Research Letters 25, 3457–3460. URL: <http://doi.wiley.com/10.1029/98GL02690>, doi:10.1029/98GL02690.

667 De La Chapelle, S., Castelnau, O., Lipenkov, V., Duval, P., 1998. Dynamic
668 recrystallization and texture development in ice as revealed by the study
669 of deep ice cores in Antarctica and Greenland. *Journal of Geophysical*
670 *Research: Solid Earth* 103, 5091–5105. URL: [http://doi.wiley.com/](http://doi.wiley.com/10.1029/97JB02621)
671 [10.1029/97JB02621](http://doi.wiley.com/10.1029/97JB02621), doi:10.1029/97JB02621.

672 Derby, B., 1992. Dynamic recrystallisation: The steady state grain
673 size. *Scripta Metallurgica et Materialia* 27, 1581–1585. URL: [https://](https://linkinghub.elsevier.com/retrieve/pii/0956716X92901488)
674 linkinghub.elsevier.com/retrieve/pii/0956716X92901488, doi:10.
675 [1016/0956-716X\(92\)90148-8](https://doi.org/10.1016/0956-716X(92)90148-8).

676 Derby, B., Ashby, M., 1987. On dynamic recrystallisation. *Scripta Metallur-*
677 *gica* 21, 879–884. URL: [https://linkinghub.elsevier.com/retrieve/](https://linkinghub.elsevier.com/retrieve/pii/0036974887903413)
678 [pii/0036974887903413](https://linkinghub.elsevier.com/retrieve/pii/0036974887903413), doi:10.1016/0036-9748(87)90341-3.

679 Duval, P., 1981. Creep and Fabrics of Polycrystalline Ice Under Shear and
680 Compression. *Journal of Glaciology* 27, 129–140.

681 Duval, P., 1985. Grain growth and mechanical behaviour of polar ice. *Annals*
682 *of Glaciology* , 3–6.

683 Duval, P., Ashby, M.F., Anderman, I., 1983. Rate-controlling processes in the
684 creep of polycrystalline ice. *Journal of Physical Chemistry* 87, 4066–4074.
685 doi:10.1021/j100244a014.

686 Duval, P., Castelnau, O., 1995. Dynamic recrystallization of

Non-peer-reviewed preprint

- 687 ice in polar ice sheets. *Journal de Physique IV* 5, 197–
688 205. URL: [http://www.scopus.com/inward/record.url?eid=2-s2.](http://www.scopus.com/inward/record.url?eid=2-s2.0-33750590172&partnerID=MN8TOARS)
689 [0-33750590172](http://www.scopus.com/inward/record.url?eid=2-s2.0-33750590172&partnerID=MN8TOARS){\&}partnerID=MN8TOARS, doi:10.1051/jp4.
- 690 Duval, P., Gac, H.L., 1980. Does the Permanent Creep-Rate of Polycrys-
691 talline Ice Increase with Crystal Size? *Journal of Glaciology* 25, 151–158.
692 doi:10.3189/s0022143000010364.
- 693 Gardner, A.S., Moholdt, G., Scambos, T., Fahnestock, M., Ligtenberg,
694 S., van den Broeke, M., Nilsson, J., 2018. Increased West Antarctic
695 and unchanged East Antarctic ice discharge over the last 7 years. *The*
696 *Cryosphere* 12, 521–547. URL: [https://tc.copernicus.org/articles/](https://tc.copernicus.org/articles/12/521/2018/)
697 [12/521/2018/](https://tc.copernicus.org/articles/12/521/2018/), doi:10.5194/tc-12-521-2018.
- 698 Goldsby, D.L., Kohlstedt, D.L., 2001. Superplastic deformation of ice: Exper-
699 imental observations. *Journal of Geophysical Research: Solid Earth* 106,
700 11017–11030. URL: <http://doi.wiley.com/10.1029/2000JB900336>,
701 doi:10.1029/2000JB900336.
- 702 Gow, A.J., Meese, D.A., Alley, R.B., Fitzpatrick, J.J., Anandakrishnan, S.,
703 Woods, G.A., Elder, B.C., 1997. Physical and structural properties of the
704 Greenland Ice Sheet Project 2 ice core: A review. *Journal of Geophysical*
705 *Research: Oceans* 102, 26559–26575. URL: [http://doi.wiley.com/10.](http://doi.wiley.com/10.1029/97JC00165)
706 [1029/97JC00165](http://doi.wiley.com/10.1029/97JC00165), doi:10.1029/97JC00165.
- 707 Gudmundsson, G.H., Paolo, F.S., Adusumilli, S., Fricker, H.A., 2019.
708 Instantaneous Antarctic ice sheet mass loss driven by thinning ice
709 shelves. *Geophysical Research Letters* 46, 13903–13909. URL: <https://doi.org/10.1029/2019GL083000>.

Non-peer-reviewed preprint

710 //onlinelibrary.wiley.com/doi/abs/10.1029/2019GL085027, doi:10.
711 1029/2019GL085027.

712 Gundestrup, N., Dahl-Jensen, D., Johnsen, S., Rossi, A., 1993. Bore-
713 hole survey at dome GRIP 1991. *Cold Regions Science and Technology*
714 21, 399–402. URL: [https://linkinghub.elsevier.com/retrieve/pii/
715 0165232X9390015Z](https://linkinghub.elsevier.com/retrieve/pii/S0165232X9390015Z), doi:10.1016/0165-232X(93)90015-Z.

716 Hall, C.E., Parmentier, E.M., 2003. Influence of grain size evolution on con-
717 vective instability. *Geochemistry, Geophysics, Geosystems* 4. URL: [http:
718 //doi.wiley.com/10.1029/2002GC000308](http://doi.wiley.com/10.1029/2002GC000308), doi:10.1029/2002GC000308.

719 Helm, V., Humbert, A., Miller, H., 2014. Elevation and elevation change
720 of Greenland and Antarctica derived from CryoSat-2. *The Cryosphere*
721 8, 1539–1559. URL: [https://tc.copernicus.org/articles/8/1539/
722 2014/](https://tc.copernicus.org/articles/8/1539/2014/), doi:10.5194/tc-8-1539-2014.

723 Higashi, A., 1978. Structure and Behaviour of Grain Boundaries in Poly-
724 crystalline Ice. *Journal of Glaciology* 21, 589–605. URL: [https://www.
725 cambridge.org/core/product/identifier/S0022143000033712/type/
726 journal_article](https://www.cambridge.org/core/product/identifier/S0022143000033712/type/journal_article), doi:10.3189/S0022143000033712.

727 Howat, I.M., Porter, C., Smith, B.E., Noh, M.J., Morin, P., 2019.
728 The Reference Elevation Model of Antarctica. *The Cryosphere* 13,
729 665–674. URL: [https://tc.copernicus.org/articles/13/665/2019/
730 doi:10.5194/tc-13-665-2019](https://tc.copernicus.org/articles/13/665/2019/).

731 Hrubby, K., Gerbi, C., Koons, P., Campbell, S., Martín, C., Hawley,
732 R., 2020. The impact of temperature and crystal orientation fabric

733 on the dynamics of mountain glaciers and ice streams. *Journal of*
734 *Glaciology* 66, 755–765. URL: [https://www.cambridge.org/core/](https://www.cambridge.org/core/product/identifier/S0022143020000441/type/journal-article)
735 [product/identifier/S0022143020000441/type/journal-article](https://www.cambridge.org/core/product/identifier/S0022143020000441/type/journal-article),
736 doi:10.1017/jog.2020.44.

737 Hvidberg, C.S., Dahl-Jensen, D., Waddington, E.D., 1997. Ice flow between
738 the Greenland Ice Core Project and Greenland Ice Sheet Project 2 bore-
739 holes in central Greenland. *Journal of Geophysical Research: Oceans* 102,
740 26851–26859. doi:10.1029/97JC00268.

741 Jacka, T., 1984. Laboratory studies on relationships between ice
742 crystal size and flow rate. *Cold Regions Science and Technology*
743 10, 31–42. URL: [https://linkinghub.elsevier.com/retrieve/pii/](https://linkinghub.elsevier.com/retrieve/pii/S0165232X84900314)
744 [0165232X84900314](https://linkinghub.elsevier.com/retrieve/pii/S0165232X84900314), doi:10.1016/0165-232X(84)90031-4.

745 Jacka, T.H., Li Jun, 1994. The steady-state crystal size of deforming ice.
746 *Annals of Glaciology* 20, 13–18.

747 Jackson, M., Kamb, B., 1997. The marginal shear stress of Ice Stream B ,
748 West Antarctica. *Journal of Glaciology* 43, 415–426.

749 Jacobson, H.P., Raymond, C.F., 1998. Thermal effects on the location of ice
750 stream margins. *Journal of Geophysical Research: Solid Earth* 103, 12111–
751 12122. URL: <http://doi.wiley.com/10.1029/98JB00574>, doi:10.1029/
752 98JB00574.

753 Jezek, K., Alley, R., Thomas, 1985. Rheology of Glacier Ice. *Science* 227,
754 1335–1337. URL: [https://www.sciencemag.org/lookup/doi/10.1126/](https://www.sciencemag.org/lookup/doi/10.1126/science.227.4692.1335)
755 [science.227.4692.1335](https://www.sciencemag.org/lookup/doi/10.1126/science.227.4692.1335), doi:10.1126/science.227.4692.1335.

Non-peer-reviewed preprint

- 756 Johnsen, S., Clausen, H.B., Dansgaard, W., Gundestrup, N.S., Hammer,
757 C.U., Andersen, U., Andersen, K.K., Hvidberg, C.S., Steffensen, P., White,
758 J., Jouzel, J., Fisher, D., 1997. The Delta 18O along the Greenland Ice
759 Core Project deep ice core and the problem of possible Eemian climatic
760 instability. *Journal of Geophysical Research* 102, 26,397 – 26,410.
- 761 Karato, S.i., 2008. *Deformation of Earth Materials: An Introduction to the*
762 *Rheology of Solid Earth*. Cambridge University Press.
- 763 Ketcham, W.M., Hobbs, P.V., 1969. An experimental determination of the
764 surface energies of ice. *Philosophical Magazine* 19, 1161–1173. doi:10.
765 1080/14786436908228641.
- 766 Kuiper, E.J.N., De Bresser, J.H., Drury, M.R., Eichler, J., Pennock, G.M.,
767 Weikusat, I., 2020. Using a composite flow law to model deformation in
768 the NEEM deep ice core, Greenland-Part 2: The role of grain size and pre-
769 melting on ice deformation at high homologous temperature. *Cryosphere*
770 14, 2449–2467. doi:10.5194/tc-14-2449-2020.
- 771 Lee, R.W., Schulson, E.M., 1988. The Strength and Ductility of Ice Under Tension. *Journal of Offshore Mechanics and Arctic Engineering* 110, 187–191. URL: <https://asmedigitalcollection.asme.org/offshoremechanics/article/110/2/187/435450/The-Strength-and-Ductility-of-Ice-Under-Tension>,
774 doi:10.1115/1.3257049.
- 777 Lhermitte, S., Sun, S., Shuman, C., Wouters, B., Pattyn, F., Wuite,
778 J., Berthier, E., Nagler, T., 2020. Damage accelerates ice shelf in-

Non-peer-reviewed preprint

779 stability and mass loss in Amundsen Sea Embayment. Proceedings
780 of the National Academy of Sciences 117, 24735–24741. URL: <http://www.pnas.org/lookup/doi/10.1073/pnas.1912890117>, doi:10.1073/
781 //www.pnas.org/lookup/doi/10.1073/pnas.1912890117, doi:10.1073/
782 pnas.1912890117.

783 Li, J.C.M., Chou, Y.T., 1970. The role of dislocations in the flow stress
784 grain size relationships. Metallurgical and Materials Transactions B 1,
785 1145. URL: <http://link.springer.com/10.1007/BF02900225>, doi:10.
786 1007/BF02900225.

787 Llorens, M.G., Griera, A., Steinbach, F., Bons, P.D., Gomez-Rivas, E.,
788 Jansen, D., Roessiger, J., Lebensohn, R.A., Weikusat, I., 2017. Dy-
789 namic recrystallization during deformation of polycrystalline ice: in-
790 sights from numerical simulations. Philosophical Transactions of the
791 Royal Society A: Mathematical, Physical and Engineering Sciences 375,
792 20150346. URL: [https://royalsocietypublishing.org/doi/10.1098/](https://royalsocietypublishing.org/doi/10.1098/rsta.2015.0346)
793 [rsta.2015.0346](https://royalsocietypublishing.org/doi/10.1098/rsta.2015.0346), doi:10.1098/rsta.2015.0346.

794 MacAyeal, D.R., 1989. Large-scale ice flow over a viscous basal sediment:
795 Theory and application to ice stream B, Antarctica. Journal of Geophysical
796 Research: Solid Earth 94, 4071–4087. URL: [http://doi.wiley.com/10.](http://doi.wiley.com/10.1029/JB094iB04p04071)
797 [1029/JB094iB04p04071](http://doi.wiley.com/10.1029/JB094iB04p04071), doi:10.1029/JB094iB04p04071.

798 Meyer, C.R., Minchew, B.M., 2018. Temperate ice in the shear
799 margins of the Antarctic Ice Sheet: Controlling processes and pre-
800 liminary locations. Earth and Planetary Science Letters 498, 17–
801 26. URL: <https://doi.org/10.1016/j.epsl.2018.06.028>[https://](https://doi.org/10.1016/j.epsl.2018.06.028)

Non-peer-reviewed preprint

802 linkinghub.elsevier.com/retrieve/pii/S0012821X18303790, doi:10.
803 1016/j.epsl.2018.06.028.

804 Millstein, J., Minchew, B., 2020. Inferring ice rheology in Antarctic ice
805 shelves using remotely-sensed surface velocity and ice thickness observa-
806 tions. AGU Fall Meeting 2020 .

807 Montagnat, M., Duval, P., 2000. Rate controlling processes in the creep of po-
808 lar ice, influence of grain boundary migration associated with recrystalliza-
809 tion. Earth and Planetary Science Letters 183, 179–186. URL: [https://](https://linkinghub.elsevier.com/retrieve/pii/S0012821X00002624)
810 linkinghub.elsevier.com/retrieve/pii/S0012821X00002624, doi:10.
811 1016/S0012-821X(00)00262-4.

812 Montési, L.G., Hirth, G., 2003. Grain size evolution and the rheol-
813 ogy of ductile shear zones: from laboratory experiments to postseismic
814 creep. Earth and Planetary Science Letters 211, 97–110. URL: [https://](https://linkinghub.elsevier.com/retrieve/pii/S0012821X03001961)
815 linkinghub.elsevier.com/retrieve/pii/S0012821X03001961, doi:10.
816 1016/S0012-821X(03)00196-1.

817 Morlighem, M., Rignot, E., Binder, T., Blankenship, D.D., Drews, R., Eagles,
818 G., Eisen, O., Ferraccioli, F., Forsberg, R., Fretwell, P., Goel, V., Green-
819 baum, J., Gudmundsson, H., Guo, J., Gelm, V., Hofstede, C., Howat, I.,
820 Humbert, A., Jokat, W., Karlsson, N., Lee, W., Matsuoka, K., Millan, R.,
821 Mouginot, J., Paden, J., Pattyn, F., Roberts, J., Rosier, S., Ruppel, A.,
822 Seroussi, H., Smith, E., Steinhage, D., Sun, B., van den Broeke, M., van
823 Ommen, T., van Wessem, M., Young, D., 2020. Deep glacial troughs and
824 stabilizing ridges unveiled beneath the margins of the Antarctic ice sheet.
825 Nature Geoscience 13, 132–137.

Non-peer-reviewed preprint

826 Mougnot, J., Scheuch, B., Rignot, E., 2012. Mapping of ice motion in
827 antarctica using synthetic-aperture radar data. *Remote Sensing* 4, 2753–
828 2767. doi:10.3390/rs4092753.

829 Ng, F., Jacka, T., 2014. A model of crystal-size evolution in polar ice masses.
830 *Journal of Glaciology* 60, 463–477. URL: [https://www.cambridge.org/
831 core/product/identifier/S0022143000205947/type/journal{\
832 }article](https://www.cambridge.org/core/product/identifier/S0022143000205947/type/journal-article), doi:10.3189/2014JoG13J173.

833 Nixon, W., Schulson, E., 1987. A Micromechanical view of the fracture
834 toughness of ice. *Le Journal de Physique Colloques* 48, C1–313–C1–
835 319. URL: <http://www.edpsciences.org/10.1051/jphyscol:1987144>,
836 doi:10.1051/jphyscol:1987144.

837 Nixon, W.A., Schulson, E.M., 1988. The Fracture Toughness of
838 Ice Over a Range of Grain Sizes. *Journal of Offshore Me-
839 chanics and Arctic Engineering* 110, 192–196. URL: [https://
840 asmedigitalcollection.asme.org/offshoremechanics/article/110/
841 2/192/435461/The-Fracture-Toughness-of-Ice-Over-a-Range-of](https://asmedigitalcollection.asme.org/offshoremechanics/article/110/2/192/435461/The-Fracture-Toughness-of-Ice-Over-a-Range-of),
842 doi:10.1115/1.3257050.

843 Pollard, D., DeConto, R.M., Alley, R.B., 2015. Potential Antarc-
844 tic Ice Sheet retreat driven by hydrofracturing and ice cliff
845 failure. *Earth and Planetary Science Letters* 412, 112–121.
846 URL: <http://dx.doi.org/10.1016/j.epsl.2014.12.035>[https://
847 linkinghub.elsevier.com/retrieve/pii/S0012821X14007961](https://linkinghub.elsevier.com/retrieve/pii/S0012821X14007961),
848 doi:10.1016/j.epsl.2014.12.035.

Non-peer-reviewed preprint

- 849 Porter, C., Morin, P., Howat, I., Noh, M.J., Bates, B., Peterman, K., Keeseey,
850 S., Schlenk, M., Gardiner, J., Tomko, K., Willis, M., Kelleher, C., Cloutier,
851 M., Husby, E., Foga, S., Nakamura, H., Platson, M., Wethington, M.J.,
852 Williamson, C., Bauer, G., Enos, J., Arnold, G., Kramer, W., Becker,
853 P., Doshi, A., D'Souza, C., Cummens, P., Laurier, F., Bojesen, M., 2018.
854 ArcticDEM. doi:10.7910/DVN/OHHUKH.
- 855 Ranganathan, M., Minchew, B., Meyer, C.R., Gudmundsson, G.H.,
856 2021. A new approach to inferring basal drag and ice rheology in ice
857 streams, with applications to West Antarctic Ice Streams. *Journal of*
858 *Glaciology* 67, 229–242. URL: [https://www.cambridge.org/core/](https://www.cambridge.org/core/product/identifier/S0022143020000957/type/journal-article)
859 [product/identifier/S0022143020000957/type/journal-article](https://www.cambridge.org/core/product/identifier/S0022143020000957/type/journal-article),
860 doi:10.1017/jog.2020.95.
- 861 Raymond, C.F., 1983. Deformation in the vicinity of ice divides. *Journal of*
862 *Glaciology* 29, 357–373. doi:10.1017/S0022143000030288.
- 863 Rignot, E., Mouginot, J., Scheuchl, B., 2017. MEaSURES InSAR-Based
864 Antarctica Ice Velocity Map, Version 2. doi:[https://doi.org/10.5067/](https://doi.org/10.5067/D7GK8F5J8M8R)
865 [D7GK8F5J8M8R](https://doi.org/10.5067/D7GK8F5J8M8R).
- 866 Rios, P.R., Siciliano Jr, F., Sandim, H.R.Z., Plaut, R.L., Padilha, A.F.,
867 2005. Nucleation and growth during recrystallization. *Materials Research*
868 8, 225–238. URL: [http://www.scielo.br/scielo.php?script=sci-arttext&](http://www.scielo.br/scielo.php?script=sci-arttext&pid=S1516-14392005000300002&lng=en&tlng=en)
869 [pid=S1516-14392005000300002&lng=en&tlng=en](http://www.scielo.br/scielo.php?script=sci-arttext&pid=S1516-14392005000300002&lng=en&tlng=en),
870 doi:10.1590/S1516-14392005000300002.
- 871 Schulson, E.M., Hibler, W.D., 1991. The fracture of ice on scales

Non-peer-reviewed preprint

895 dron collapse, Vatnajökull ice cap, Iceland. *Journal of Glaciol-*
896 ogy 66, 1024–1033. URL: [https://www.cambridge.org/core/
897 product/identifier/S0022143020000659/type/journal-article,](https://www.cambridge.org/core/product/identifier/S0022143020000659/type/journal-article)
898 doi:10.1017/jog.2020.65.

899 Urai, J., Means, W., Lister, G., 1995. Dynamic Recrystallization of Minerals.
900 Geophysical Monograph Series 36, 332–347.

901 Van der Wal, D., Chopra, P., Drury, M., Gerald, J.F., 1993. Relationships
902 between dynamically recrystallized grain size and deformation conditions
903 in experimentally deformed olivine rocks. *Geophysical Research Letters*
904 20, 1479–1482. doi:10.1029/93GL01382.

905 Van Wessem, J.M., Reijmer, C.H., Morlighem, M., Mougintot, J., Rignot,
906 E., Medley, B., Joughin, I., Wouters, B., Depoorter, M.A., Bamber, J.L.,
907 Lenaerts, J.T., Van De Berg, W.J., Van Den Broeke, M.R., Van Meijgaard,
908 E., 2014. Improved representation of East Antarctic surface mass balance
909 in a regional atmospheric climate model. *Journal of Glaciology* 60, 761–
910 770. doi:10.3189/2014JoG14J051.

911 Vaughan, D.G., 1993. Relating the occurrence of crevasses to surface strain
912 rates. *Journal of Glaciology* 39, 255–266. URL: [https://www.cambridge.
913 org/core/product/identifier/S0022143000015926/type/journal-article,](https://www.cambridge.org/core/product/identifier/S0022143000015926/type/journal-article)
914 doi:10.1017/S0022143000015926.

915 Webster, G.A., 1966a. A widely applicable dislocation model of creep. *Philo-*
916 sophical Magazine 14, 775–783. doi:10.1080/14786436608211971.

Non-peer-reviewed preprint

917 Webster, G.A., 1966b. In support of a model of creep based on dislo-
918 cation dynamics. *Philosophical Magazine* 14, 1303–1307. doi:10.1080/
919 14786436608224296.

920 Wingham, D.J., Wallis, D.W., Shepherd, A., 2009. Spatial and temporal
921 evolution of Pine Island Glacier thinning, 1995-2006. *Geophysical Research*
922 *Letters* 36, 5–9. doi:10.1029/2009GL039126.